ACCOUNTS of chemical research

Article

pubs.acs.org/accounts

Metal Hybrid Nanoparticles for Catalytic Organic and Photochemical Transformations

Hyunjoon Song*

Department of Chemistry, Korea Advanced Institute of Science and Technology, 291 Daehak-ro, Yuseong-gu, Daejeon, 305-701, Korea

Center for Nanomaterials and Chemical Reactions, Institute for Basic Science, 291 Daehak-ro, Yuseong-gu, Daejeon, 305-701, Korea

CONSPECTUS: In order to understand heterogeneous catalytic reactions, model catalysts such as a single crystalline surface have been widely studied for many decades. However, catalytic systems that actually advance the reactions are three-dimensional and commonly have multiple components including active metal nanoparticles and metal oxide supports. On the other hand, as nanochemistry has rapidly been developed and been applied to various fields, many researchers have begun to discuss the impact of nanochemistry on heterogeneous catalysis. Metal hybrid nanoparticles bearing multiple components are structurally very close to the actual catalysts, and their uniform and controllable morphology is suitable for investigating the relationship between the structure and the catalytic properties in detail.

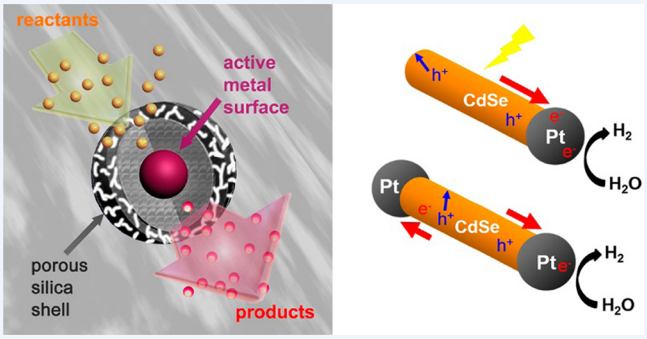

In this Account, we introduce four typical structures of metal hybrid nanoparticles that can be used to conduct catalytic organic and photochemical reactions. Metal@silica (or metal oxide) yolk−shell nanoparticles, in which metal cores exist in internal voids surrounded by thin silica (or metal oxide) shells, exhibited extremely high thermal and chemical stability due to the geometrical protection of the silica layers against the metal cores. The morphology of the metal cores and the pore density of the hollow shells were precisely adjusted to optimize the reaction activity and diffusion rates of the reactants. Metal@metal oxide core−shell nanoparticles and inverted structures, where the cores supported the shells serving an active surface, exhibited high activity with no diffusion barriers for the reactants and products. These nanostructures were used as effective catalysts for various organic and gas-phase reactions, including hydrogen transfer, Suzuki coupling, and steam methane reforming.

In contrast to the yolk− and core−shell structures, an asymmetric arrangement of distinct domains generated acentric dumbbells and tipped rods. A large domain of each component added multiple functions, such as magnetism and light absorption, to the catalytic properties. In particular, metal−semiconductor hybrid nanostructures could behave as effective visible photocatalysts for hydrogen evolution and CO oxidation reactions. Resulting from the large surface area and high local concentration of the reactants, a double-shell hollow structure showed reaction activities higher than those of filled nanoparticles. The introduction of plasmonic Au probes into the Pt−CdS double-shell hollow particles facilitated the monitoring of photocatalytic hydrogen generation that occurred on an individual particle surface by single particle measurements.

Further development of catalysis research using well-defined metal hybrid nanocatalysts with various in situ spectroscopic tools provides a means of maximizing catalytic performances until they are comparable to or better than those of homogeneous catalysts, and this would have possibly useful implications for industrial applications.

1. INTRODUCTION

Metal nanoparticles have been used as catalysts for various organic reactions over the past decade.[1−3] Although some debate as to whether active species are heterogeneous or organometallic complexes remains unresolved, numerous metal nanoparticles can reportedly serve as an effective surface on which the actual reaction occurs. Metal nanoparticles have the advantages of easy and complete separation from the reaction mixture, excellent recyclability, and high activity comparable to that of homogeneous counterparts.[4]

In addition to active metal nanoparticles, most industrially valuable catalysts consist of additional components such as metal oxide supports. To investigate the reaction process and its mechanisms within these types of multicomponent systems,[5] the catalyst structure should be precisely defined and highly resolved,[6] with the model reactions carried out under well-controlled conditions.[7,8] In this regard, metal hybrid nanoparticles are perfectly matched to these conditions given their structural dimensions and good uniformity. Moreover, recent developments in nanoparticle synthesis have provided a large pool of hybrid nanostructures with multiple components, offering a wide structural selection of suitable components.[9]

Received: November 6, 2013
Published: March 2, 2015

DOI: 10.1021/ar500411s
Acc. Chem. Res. 2015, 48, 491−499

The structural arrangement between distinct components is as important as the components themselves. What would be the best morphology of catalysts for any specific reaction? In a single component system, a type of morphology with high index surface facets tends to increase the reaction activity per area but decrease its thermodynamic stability.[10] A multicomponent system is more sophisticated in terms of this aspect; therefore, a careful design of the catalyst structure is required. Actual metal catalysts are three-dimensional materials, and there are several well-defined structural models that may be ideal for catalysis purposes.[6]

In this Account, we classified major representative structures of metal hybrid nanoparticles by their shape and morphology (Figure 1) and demonstrated their catalytic performances. The

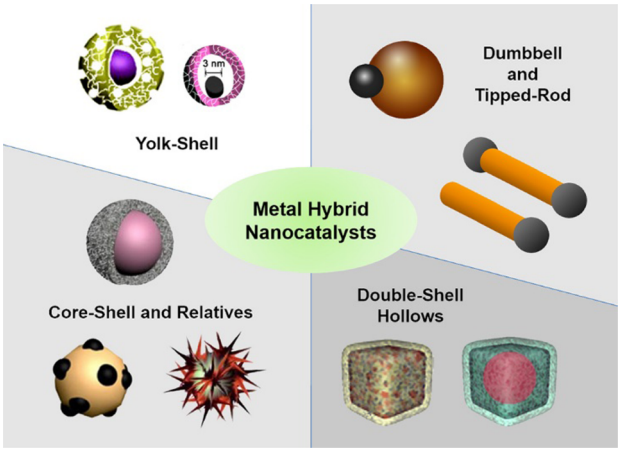

Figure 1. Metal hybrid nanoparticles as heterogeneous catalysts.

symmetric deposition of silica (or metal oxide) onto metal particles yields common core–shell nanoparticles, and subsequent chemical treatment leads to the formation of a yolk–shell structure. The inverted core–shell structures are also important for catalysis, such as core–particle and core–branch nanoparticles, in which the active components are exposed outward. The asymmetric deposition of an additional component onto the metal particles generates a dumbbell-like structure, and selective metal deposition onto nanorods provides a tipped-rod morphology. Instead of active metal cores, a double-shell hollow structure can also behave as an effective catalyst due to its high surface area and the pores on its walls. Each of these morphologies has pros and cons as a heterogeneous reaction catalyst, but in some particular cases, strongly enhanced reaction properties are realized, such as good activity, selectivity, or recyclability. Given these well-defined structures, a reaction with a metal hybrid nanocatalyst can provide essential information with which to explore the correlation between the structure and the catalytic properties.

2. METAL@SILICA OR METAL OXIDE YOLK–SHELL NANOPARTICLES

Metal@silica yolk–shell nanoparticles (or nanorattles) comprise metal cores and silica hollow shells.[11] The major synthetic scheme is the concentric polymerization of silica on the surface of metal nanoparticles, followed by the partial dissolution of metal cores.[12] The individual metal cores are completely surrounded by silica shells but are not in direct contact with the silica. As a result, the entire metal surface can be exposed to the reaction mixture, which is a major difference with regard to core–shell nanoparticles. Since Mulvaney et al. initially reported,[12] many researchers have developed new synthetic methods to construct core and shell structures with internal void space[13] and used them as a drug delivery vehicle, Raman scattering substrate, and anode materials in Li-ion battery.[14] In particular, the yolk–shell structure is regarded as an ideal model of a heterogeneous catalyst system. The metal@silica yolk–shell particles conceptually mimic the general structure of a bifunctional heterogeneous catalyst, which contains active metal nanoparticles and a silica support with a high surface area.[15] During the reaction, the reactants diffuse inside through the pores of the shells, with the reaction occurring on the metal core surface exposed to the void. The resulting products diffuse out through the pores. All of the reactions occur inside the silica shells; therefore, this yolk–shell structure behaves as a miniaturized version of a bulk reactor and is thus referred to as a "nanoreactor".[16]

The strong point of this yolk–shell nanostructure as a heterogeneous catalyst is its controllability. The size and surface structure of the metal cores, the thickness and pore density of the hollow shells, and the volume of the inner voids are readily adjustable under the appropriate synthesis conditions. The metal core size can be reduced by repeating the etching process on the original core–shell nanoparticles. For instance, the repeated dissolution of the Au cores in Au@SiO_2 yolk–shell nanoparticles by KCN diminished the average core diameter from 120 nm for the core–shell to 104, 67, and 43 nm for the yolk–shell structures (Figure 2).[17] The resulting rate constant

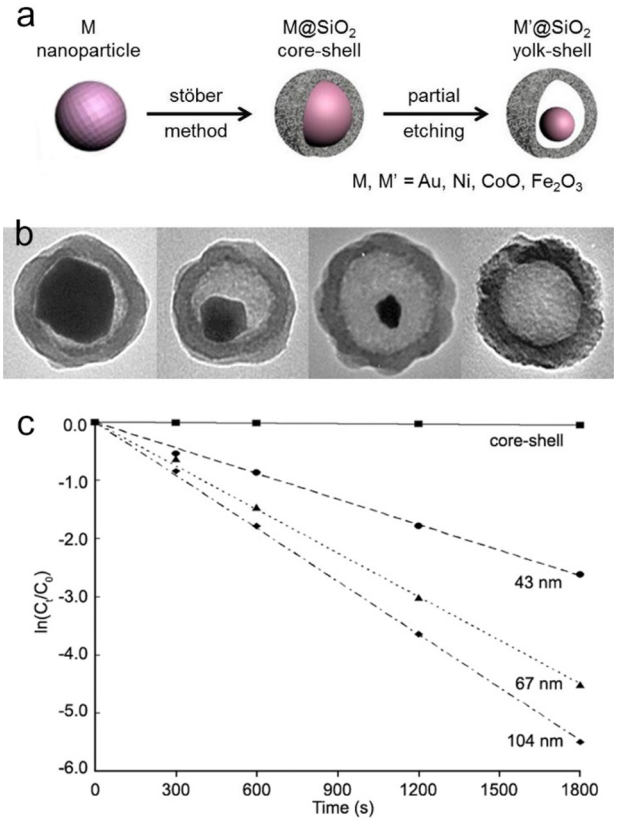

Figure 2. (a) Synthesis of metal and metal oxide@SiO_2 yolk–shell nanoparticles. (b) TEM images of individual Au@SiO_2 yolk–shell nanoparticles with different core sizes. (c) Plot of $\ln(C_t/C_0)$ versus time for each nanocatalyst, where C_t and C_0 denote the *p*-nitrophenol concentrations at time *t* and 0. Adapted with permission from ref 17.

DOI: 10.1021/ar500411s
Acc. Chem. Res. 2015, 48, 491–499

for the reduction of *p*-nitrophenol by $NaBH_4$ decreased from 1.4×10^{-2} to 3.9×10^{-3} s^{-1},[18] but the turnover frequency (TOF) on the surface atoms increased significantly from 6.6 to 36 s^{-1}, as the Au core size was reduced (Figure 2c). These trends are consistent with the fact that small Au cores have a large surface area with highly active sites.

To optimize the reactivity, the particle size should be reduced to a range of a few nanometers to maximize the active area on the surface. To this end, a microemulsion method in organic media is suitable for silica coating of tiny metal nanoparticles, whereas the Stöber method in alcohol is only effective for particles more than 10 nm in size (Figure 3). With silica coating

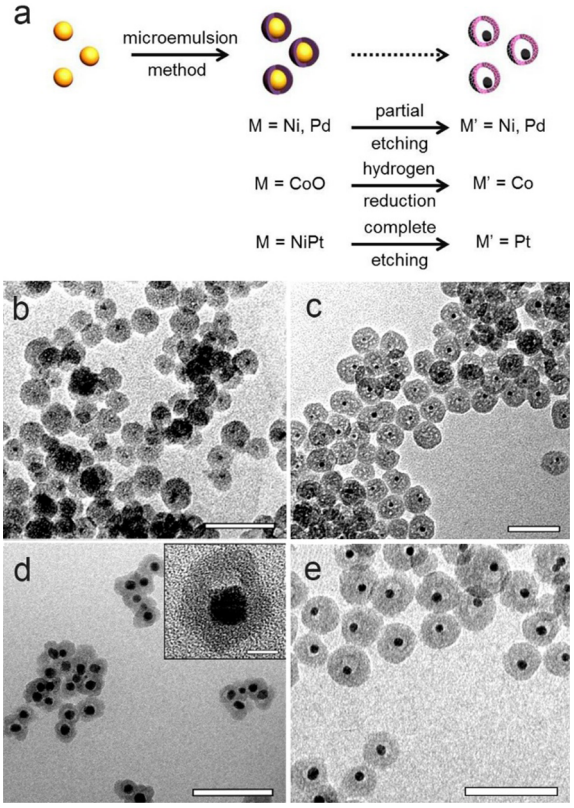

Figure 3. (a) Synthesis of metal and metal oxide@SiO_2 yolk–shell nanoparticles via a microemulsion method. TEM images of (b) Ni@SiO_2, (c) Pd@SiO_2, (d) Co@SiO_2, and (e) Pt@SiO_2 yolk–shell nanoparticles. The bars represent (b,c,e) 50 nm, (d) 100 nm, and (inset) 20 nm. Adapted with permission from refs 19, 20, 24, and 25.

via a microemulsion method and the partial etching of the metal cores, the resulting Ni@SiO_2 yolk–shell nanoparticles had the total average diameter of 17 nm with an average core size of 2.9 nm.[19] Pd@SiO_2 yolk–shell nanoparticles with tiny Pd cores were also synthesized using this method (Figure 3c).[20]

The pore density of the shells directly affects the diffusion rates of the reactants approaching active sites and eventually the activity of diffusion-controlled reactions. During the silica coating process of Au@SiO_2 yolk–shell nanoparticles, a different amount of the long-alkyl-chain siloxane octadecyltrimethoxysilane (C_{18}TMS) was introduced.[21] After selective etching of Au cores and a calcination step, the diffusion coefficient through the shells increased by 3.6 times from 5.9×10^{-19} to 2.1×10^{-18} m^2 s^{-1}, and the TOF of *o*-nitroaniline reduction with $NaBH_4$ increased by 6.9 times from 5.1 to 35 s^{-1}. In Pd@SiO_2 core–shell nanoparticles, the addition of Ni salts converted the silica surface into branched nickel phyllosilicate, and with the removal of the silica residue, Pd@nickel phyllosilicate yolk–shell nanoparticles with highly porous shells were uniformly obtained.[22] This catalyst exhibited a strong correlation of the total pore volume and the reaction activity in Suzuki coupling reactions.

With regard to the reaction properties, the yolk–shell nanoparticles have a remarkable impact on sintering resistance and recyclability characteristics due to their unique structure. The metal cores in the metal@SiO_2 yolk–shell nanoparticles are completely isolated from their neighbors by silica layers and are thus extremely robust against particle sintering, even at a temperature higher than that of the surface melting point.[7] Ni@SiO_2 yolk–shell nanoparticles were employed as an excellent model catalyst system for steam methane reforming (Figure 4).[23] Under the reforming conditions at 973 K, the yolk–shell

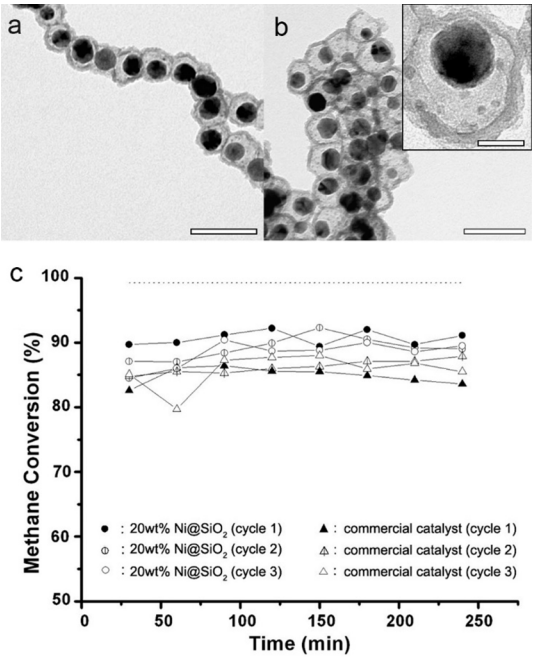

Figure 4. (a, b) TEM images of Ni@SiO_2 yolk–shell nanocatalysts. (c) Methane conversion versus time at 973 K in the presence of Ni@SiO_2 yolk–shell and commercial catalysts. The bars represent (a,b) 100 nm and (inset) 20 nm. Adapted with permission from ref 23.

catalysts exhibited a constant methane conversion yield of >90% for 4 h, nearly approaching a theoretically maximum value, and they were still active after three rounds of recycling without a loss of their methane conversion. This level of catalytic performance is comparable to those of state-of-the-art commercial catalysts (Figure 4c).

Stability is a critical issue, even in solution-phase reactions, because freestanding catalyst particles are easily agglomerated when they are used in reactions. Moreover, surface passivation by surfactants intensively blocks the active sites and lowers the reactivity. The yolk–shell nanoparticles have clean metal surfaces without surfactants after a calcination process and are controversially highly stable against agglomeration due to their protective silica layers. As a result, the reaction temperature can be increased without considering the catalyst stability. The TOF was measured to be 6000 h^{-1} when using Ni@SiO_2 yolk–shell nanocatalysts for the hydrogen transfer of acetophenone;[19] this value was 1 order of magnitude larger

DOI: 10.1021/ar500411s
Acc. Chem. Res. 2015, 48, 491–499

than those (100−500 h^{-1}) of heterogeneous Ni catalysts. In the Suzuki coupling reactions of bromobenzene with phenylboronic acid, Pd@SiO_2 yolk−shell nanocatalysts exhibited an initial TOF of 78000 h^{-1},[20] which was one of the best activity levels reported for supported Pd nanocatalysts. All reactions were recycled several times without a significant loss of the activity, confirming the superior stability of the metal@silica yolk−shell framework.

The yolk−shell morphology has many features that are appropriate for catalyst applications; however, several drawbacks remain. During the synthetic process, the partial etching of the metal cores is wasteful, particularly for expensive noble metals such as Au and Pt. To decrease the use of these materials, several synthetic processes have been developed. The metal core size was reduced by means of hydrogen reduction of metal oxides or by the partial etching of metal alloys (Figure 3a). The CoO cores in CoO@SiO_2 core−shell nanoparticles were shrunk to the Co cores, which form Co@SiO_2 core−shell nanoparticles by hydrogen reduction (Figure 3d),[24] and a Pt@SiO_2 yolk−shell morphology was generated from the NiPt@SiO_2 core−shell structure by acid treatment without a loss of Pt (Figure 3e).[25] The manipulation of silica shells is even more effective, including surface-protected etching[26] and a soft-template approach using special types of surfactants.[27]

To facilitate additional functions on the shells, various metal oxides, polymers, and carbon can be utilized.[28,29] Among metal oxides, porous TiO_2 and ZrO_2 shells exhibited surprising activities in CO oxidation,[30] and the TiO_2 shell behaved as an efficient photocatalyst in Au@TiO_2 yolk−shell nanoparticles.[31]

3. METAL−METAL OXIDE CORE−SHELL NANOPARTICLES AND RELATIVES

Metal@silica and metal oxide core−shell nanoparticles have been investigated as excellent model catalysts for high temperature reactions in the gas phase. Pt@SiO_2 and Pd@CeO_2 core−shell nanocatalysts exhibited high activity and thermal stability for ethylene hydrogenation and methane oxidation, respectively.[32,33] In these catalysts, the metal cores were accessible through the mesopores in the silica or through gaps between the metal oxide grains. There were no significant effects observed regarding the reaction rates of small molecules; however, if the reactants and products are either sterically hindered or in a liquid phase, inorganic shells behave as diffusion barriers and eventually lower the reaction activity. In order to overcome this limitation, one potential design is an inverted core−shell structure in which the core intensively anchors the shell structure while the shell serves as an active catalyst. The inverted structure can be yielded by chemical transformation of metal cores from the original core−shell nanoparticles or simply formed by the deposition of metal (or metal oxide) components on the surface of metal oxide particles. In this case, the interaction between the distinct components is potentially strong due to the formation of metal−oxygen bonds at the interface.

A new core−particle morphology was generated by sequential chemical reactions from Ni@SiO_2 core−shell nanoparticles (Figure 5a).[34] Treatment with a weak base led to a conversion from core−shell to spherical with needle-like thin branches of Ni phyllosilicate. After H_2 reduction, the morphology changed to form a SiO_2−Ni core−particle structure. Although the Ni particles were exposed on the surface, they were extremely stable against particle sintering, even after treatment at 973 K for 10 h under a hydrogen

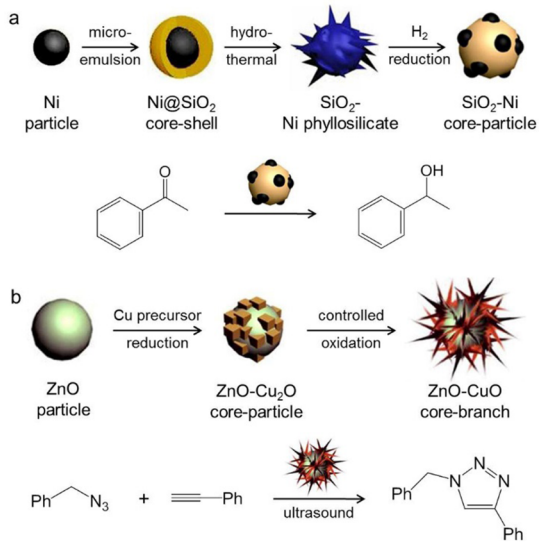

Figure 5. (a) Synthesis of the SiO_2−Ni core−particle morphology for catalytic hydrogen transfer reactions. (b) Synthesis of the ZnO−CuO core−branch morphology for ultrasound-assisted azide−alkyne cycloaddition reactions. Adapted with permission from refs 34 and 35.

environment. These particles catalyzed the hydrogen transfer of acetophenone with a 1-phenylethanol in 93% yield without byproducts within 1 h.

Another example with branches having high energy surface facets was demonstrated in the ZnO−CuO core−branch morphology (Figure 5b). The reduction of a Cu precursor on polycrystalline ZnO nanospheres formed a ZnO−Cu_2O core−particle structure. Under controlled oxidation with NaOH, the Cu_2O cubes were transformed into thin CuO branches, yielding ZnO−CuO core−branch nanoparticles. These particles were utilized as a heterogeneous catalyst for cycloaddition reactions of benzyl azide and phenylacetylene to yield 1,4-disubstituted 1,2,3-triazoles. The conversion yield was measured to be 47% for 3 h, and the yield increased to complete conversion within 10 min upon the application of low-power sonication. During the reaction, ultrasonic irradiation activated the Cu(II) surfaces, which were reduced to Cu(I) by the reaction with phenylacetylene via the formation of Cu(II)-acetylide, with the Cu(I) surface actually carrying out the catalytic cycloaddition cycle.[35] The branches of the catalyst sufficiently endured reaction recycling five times due to the strong interaction between the CuO branches and the ZnO cores.

4. ACENTRIC DUMBBELLS AND TIPPED RODS

The seed-mediated growth of multiple components commonly produces highly symmetric morphologies such as a core−shell structure, but with precise control of the growth kinetics, asymmetric structures can be obtained. Xu et al. successfully produced heterodimers bearing two distinct nanospheres at a liquid−liquid interface,[36] and Sun et al. developed general synthetic methods that could be used to produce noble metal−metal oxide dumbbell-like particles via a solvothermal process in an organic phase.[37] In the presence of metal seeds, an adjustment of the surface capping agent concentration changed the metal−Fe_3O_4 morphology from a concentric yolk−shell to acentric core−shell and dumbbell-like structures (Figure 6).[38] These dumbbell structures have a major advantage in that they offer multiple functions arising from two distinct domains. In metal−magnetic oxide dumbbells, a magnetic property is

DOI: 10.1021/ar500411s
Acc. Chem. Res. 2015, 48, 491−499

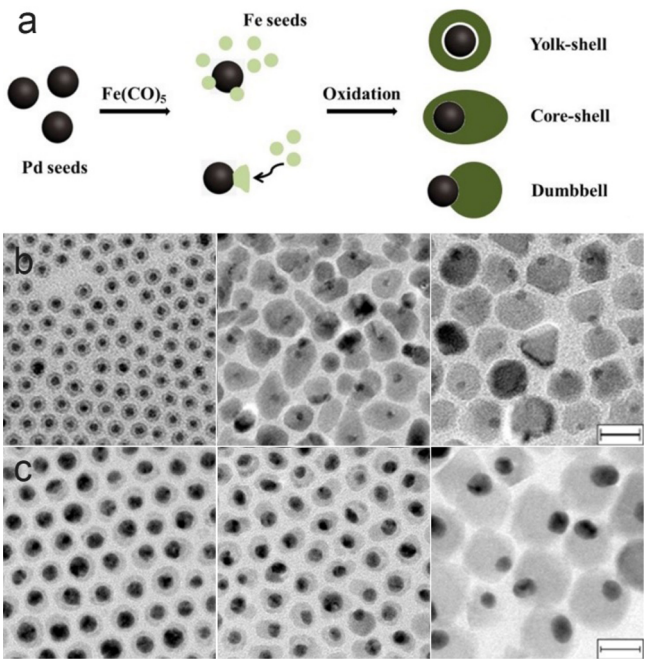

Figure 6. (a) Synthesis of metal–Fe_3O_4 hybrid nanoparticles. TEM images of concentric yolk–shell, acentric core–shell, and dumbbell morphologies of (b) Pd–Fe_3O_4 and (c) Au–Fe_3O_4 nanoparticles. The bars represent 20 nm. Adapted with permission from ref 38.

coupled with the original metallic features in a single structure.[39] In a catalytic application, catalyst particles could be simply and clearly separated from the reaction mixture by applying a magnetic field. Another important aspect of these dumbbells is the full exposure of the active surface on the catalyst, which overcomes the low diffusion rates in the yolk– and core–shell catalysts. Catalyzed by Pd@Fe_3O_4 dumbbells, the Suzuki coupling reaction of phenylboronic acid and iodobenzene produced biphenyl in a quantitative yield at 0.5% Pd loading for 12 h, whereas Pd@Fe_3O_4 yolk–shell nanoparticles only reached a 34% yield.[38] Enhancement of the catalytic activity in CO oxidation reactions was also observed in metal–Fe_3O_4 dumbbells, due to the strong interaction at the epitaxial heterojunction interface.[37]

A tipped rod structure, semiconducting rods decorated with metal tips, was originally established by Banin et al.,[40,41] and this morphology is expected to be an ideal photocatalyst.[42] Single and double Pt-tipped CdSe nanorods were demonstrated as a model catalyst for the photochemical production of hydrogen (Figure 7a,b).[43] The interface between the two components was very important to anchor the Pt tips and construct a good electronic junction on the CdSe surface, which was evidenced by the complete quenching of fluorescence signals. Under visible light irradiation, the hydrogen evolution rate reached a nearly constant value after an induction period of 30 min. Unexpectedly, the maximum rate of hydrogen evolution for the single-tipped rods (145 μmol h^{-1}) was twice as large as that of the double-tipped rods (78 μmol h^{-1}), although the Pt loading in the former case was only half that of the latter case (Figure 7c). In this catalytic system, electrons excited by the irradiation of visible light suddenly quenched into the metal tips and transferred to water generating hydrogen molecules. Holes in the valence band of the CdSe nanorods were moved to the surface and consumed by sacrificial reagents. Apparently, high reactivity of a single-

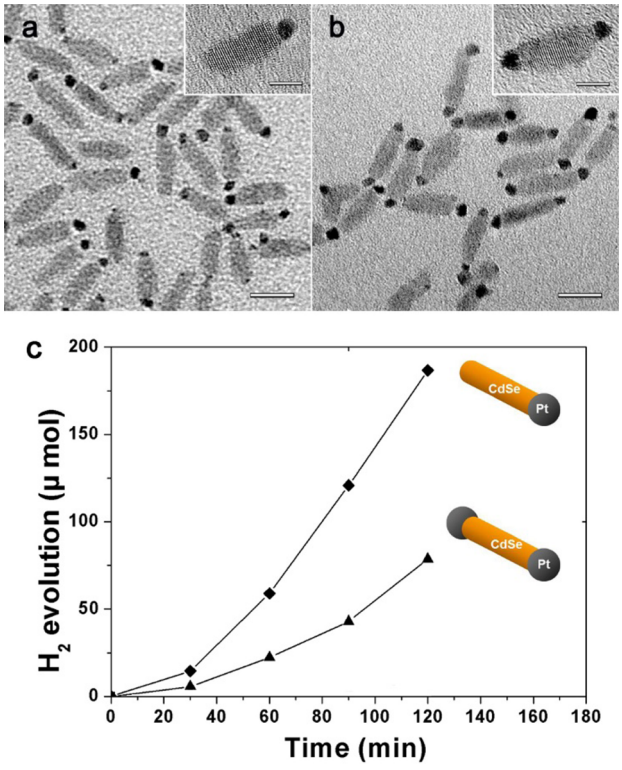

Figure 7. TEM images of (a) single- and (b) double-Pt tipped CdSe nanorods. (c) Time course of H_2 evolution by single- and double-tipped nanorods. The bars represent (a, b) 10 nm and (insets) 5 nm. Adapted with permission from ref 43.

tipped structure indicates that a unidirectional arrangement of the metal and semiconductor domains is critical for good photocatalytic efficiency. The single-tipped CdSe nanorods have a tip region that is directly open to the sacrificial reagents, where hole transfer favorably occurs. However, the Pt domains of the double-tipped structure block the effective hole transfer through the active tips, leading to the low activity of hydrogen generation.

The single and double Pt-tipped CdSe nanorods were also used for photocatalytic CO oxidation.[44] The TOF value of the double-tipped rods under light irradiation was significantly larger than that in the dark at any temperature. The catalytic activity increased in a linear fashion as the light intensity (or photon flux) increased. Importantly, the catalyst when irradiated with light with a high photon energy (2.0 eV < $h\nu$ < 3.0 eV) was twice as active for CO oxidation compared with when it was irradiated with light with a low photon energy (1.0 eV < $h\nu$ < 2.0 eV). This experiment proved that hot electrons generated by photons with energy higher than the bandgap of the CdSe rods enhanced the CO oxidation reaction on Pt metals. It was proposed that electron–hole pairs were generated on the CdSe region and the hot electrons went over the interface and were irreversibly injected to the Pt surface. Other metal-tipped semiconducting nanorods, including Pt-tipped CdSe nanonets[45] and Pt-tipped CdS nanorods,[46] were also investigated as catalysts for dye reduction and hydrogen production reactions.

5. DOUBLE-SHELL HOLLOWS

A hollow or cage structure with an internal cavity and a thin wall is of interest owing to its sufficiently large surface area and

DOI: 10.1021/ar500411s
Acc. Chem. Res. 2015, 48, 491–499

good electrical connection over the entire surface. The inner surface of the hollows is accessible by reagents that diffuse through the pores and defects of the walls.[47] It was reported that Au nanocages exhibited high activity for *p*-nitrophenol reduction by $NaBH_4$ compared with filled nanoparticles, due to the much higher surface area and ultrathin walls.[48] For hybrid nanostructures, double-wall hollow nanoparticles bearing distinct inner and outer shells were synthesized by means of controlled Galvanic replacement. A kinetic analysis using the plasmon shifts of the Au shells indicated that the reaction took place within the cavity of the hollow structure with high activity.[49]

These features of the double hollow structure enabled the catalytic system to be investigated at a single particle resolution. In recent studies, the SPR signals of individual particles could be resolved up to the single particle level. The use of dark-field microscopic images and numerical simulations made it possible to monitor the reactions occurring on the metallic surfaces.[50−52] To conduct the single particle SPR measurement, most important is the introduction of plasmon probes into heterogeneous catalytic systems. As a model heterogeneous reaction, the photocatalytic decomposition of lactic acid into pyruvic acid and hydrogen gas was chosen in the presence of a platinized cadmium sulfide (Pt/CdS) catalyst. In order to introduce plasmonic Au probes onto the Pt/CdS catalysts, two catalyst structures were designed, in which either the Au domains formed an alloy with Pt sites (AuPt/CdS hollow cubes; Figure 8a) or the Au cores were inserted into the cavity and separated from the Pt sites (Au@Pt/CdS cubes; Figure 8b).[53] In these model catalysts, photoelectrons, which were generated by photons coincident with the CdS bandgap, transferred to the Pt sites and reacted with protons to produce hydrogen molecules inside the cavity. By means of single particle dark-field spectroscopy, the SPR peak of the Au probe in that cavity was monitored as the reaction progressed on individual catalyst particles. For ten individual AuPt/CdS hollow cubes, all particles exhibited plasmon band shifts similar to the lower wavelengths due to the effective hydrogen evolution that took place. From a simulation of the first-order kinetics, the reaction rate on the catalyst surface, *k*, was analyzed to be 9.5×10^{-6} M^{-1} min^{-1}, and the average rate of hydrogen generation in the initial state was 1500 molecules per minute on a single catalyst particle. The reaction activities of individual Au@Pt/CdS cubes were close to those of the AuPt/CdS hollow cubes. Among these individual particles, seven out of 20 exhibited reverse red shifts of the extinction peaks at certain reaction times (Figure 8c,d), due to the saturation and leaking out of hydrogen gas from the inside cavity of the hollow shells at a certain time. Given this information, the diffusion coefficients through the hollow walls were calculated to be $(1.2−3.7) \times 10^{-19}$ m^2 s^{-1}. Another notable feature was that all individual Au@Pt/CdS cubes showed initial delay times of 3−12 s (Figure 8d), which were converted into the distance between the Pt sites and the Au cores, with the average being 20.3 nm.

This single particle measurement has strong points when used as an in situ analysis under actual reaction conditions without a particular reactant. For advanced reaction monitoring, time-resolved techniques using laser pulses would achieve molecular level detection,[51] and an electrochemical analysis would additionally explore the charge distribution and mass change on an individual particle.[54]

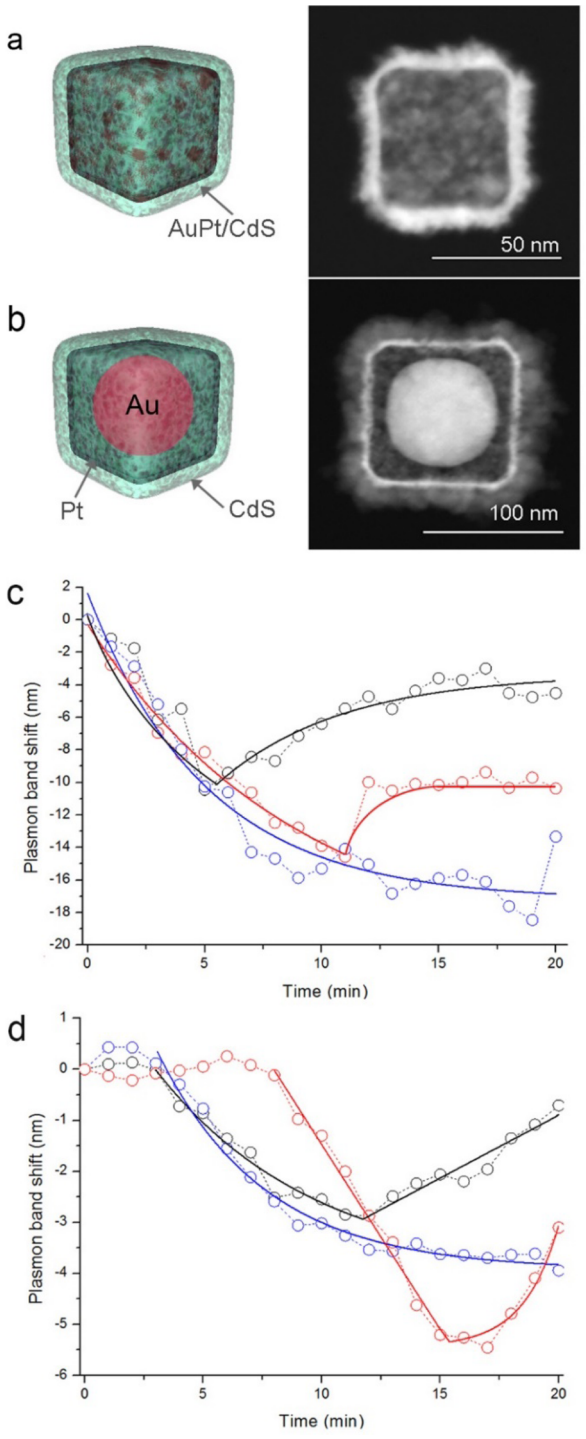

Figure 8. High-angle annular dark-field-scanning electron microscopy (HAADF-STEM) images of (a) AuPt/CdS hollow cubes and (b) Au@Pt/CdS cubes. Plasmon band shifts during the reaction progress of three individual (c) AuPt/CdS hollow cubes and (d) Au@Pt/CdS cubes. Adapted with permission from ref 53.

6. CONCLUDING REMARKS

In this Account, we demonstrated well-defined colloidal metal hybrid nanoparticles as three-dimensional model catalysts for organic and photochemical reactions. Yolk−shell nanoparticles showed excellent structural controllability and reaction activity with remarkable sinter resistance. The limit of diffusion for the reactants could be overcome by an inverted core−shell

DOI: 10.1021/ar500411s
Acc. Chem. Res. 2015, 48, 491−499

structure, the cores of which anchored the highly active branches. Asymmetric deposition of additional components into the original structure generated acentric dumbbells and tipped rods, which provided multiple functions arising from each component. The structural directionality of the tipped rods led to high efficiency of photocatalytic hydrogen generation. The double-shell hollows showed high activity compared with filled nanoparticles, enabling the monitoring of the photocatalytic reactions in situ at the single particle level.

Although these metal hybrid nanoparticles now more closely resemble real heterogeneous catalytic systems, there remain numerous challenges to explore. The most significant topic in the catalysis field is the achievement of extreme regio- and stereoselectivity for desired reactions.[7,55] By mimicking organometallic catalysts with specifically designed ligands, the heterogeneous catalysts facilitated regioselective reactions using surface-coordinating ligands.[56] However, these catalytic systems are complicated when attempting to analyze their mechanisms and intermediate structures; thus, further progress of the development of these reactions has been restricted. The combination of a well-defined catalyst morphology and in situ spectroscopic measurements may provide critical evidence with regard to these issues.

Another limitation of the current research is the generation of a charged surface in a heterogeneous system. All metal nanoparticles utilized in organic reactions thus far have had neutral metal surfaces (metal(0)), although the most active organometallic species had formal charges such as Pd(II) and Pt(IV). Recently, Toste and Somorjai reported a series of results that the oxidation of metal particle surfaces by $PhICl_2$ yielded a stable charged phase in nonpolar solvents,[57] with organic transformations occurring with high activity and selectivity as well as good recyclability.[58] We have also generated a highly Lewis-acidic Pd(IV) surface using $PhICl_2$ and *N*-chlorosuccinimide, showing high reactivity and superior stability for hydroalkoxylation reactions.[59]

What else do we expect with regard to such nanostructured catalysts? Departing from the simple mimicking of homogeneous catalytic systems, the uniqueness of heterogeneous systems must be fully explored. A tandem catalyst design using nanocrystal layers is an excellent example in this area. Assembled nanocrystal layers of CeO_2 and Pt on a silica substrate successfully catalyzed two sequential reactions of methanol decomposition and ethylene hydrogenation.[60] This approach can be extended to various sequential organic transformation reactions with the use of metal hybrid nanocatalysts bearing multiple domains with distinct activities. Lastly, several researchers have serious concerns about the contribution of such model catalysts to actual industrial processes. Even if these catalyst designs cannot directly be applied to industry, related research must at least provide a better understanding of catalyst behaviors and develop important concepts with which to enhance the catalytic properties of real systems. Xia et al. employed the concept of a porous silica coating to supported Pt catalysts on TiO_2, maximizing their sinter resistance in high temperature reactions.[61] More studies of the relationship between the structure and catalytic properties using metal hybrid nanoparticles will pave the way to the establishment of ideal heterogeneous catalyst systems that can yield desired products with high regio- and stereoselectivity, together with the advantages of extreme activity, thermal stability, and recyclability.

AUTHOR INFORMATION

Corresponding Author

*E-mail: hsong@kaist.ac.kr.

Funding

This work was supported by IBS-R004-D1 and the National Research Foundation of Korea (NRF) funded by the Korea Government (MSIP; 2012-005624, R11-2007-050-00000-0).

Notes

The authors declare no competing financial interest.

Biography

Hyunjoon Song received B.S., M.S., and Ph.D. degrees from the Department of Chemistry at Korea Advanced Institute of Science and Technology (KAIST) in 1994, 1996, and 2000. He worked as a postdoctoral fellow at KAIST and at University of California, Berkeley, until 2004. He was affiliated as assistant professor in 2005, and was promoted to associate and then to full professor in 2008 and 2014, respectively, in the Department of Chemistry at KAIST. His research interests are the morphology control of metal hybrid nanoparticles and their applications for surface plasmon monitoring, energy catalysts, and electronic materials.

REFERENCES

(1) Smith, G. V.; Notheisz, F. *Heterogeneous Catalysis in Organic Chemistry*; Academic Press: San Diego, CA, 1999.

(2) Roucoux, A.; Schulz, J.; Patin, H. Reduced transition metal colloids: A novel family of reusable catalysts? *Chem. Rev.* **2002**, *102*, 3757−3778.

(3) Chng, L. L.; Erathodiyil, N.; Ying, J. Y. Nanostructured catalysts for organic transformations. *Acc. Chem. Res.* **2013**, *46*, 1825−1837.

(4) Astruc, D.; Lu, F.; Aranzaes, J. R. Nanoparticles as recyclable catalysts: The frontier between homogeneous and heterogeneous catalysis. *Angew. Chem., Int. Ed.* **2005**, *44*, 7852−7872.

(5) Somorjai, G. A.; Contreras, A. M.; Montano, M.; Rioux, R. M. Clusters, surfaces, and catalysis. *Proc. Natl. Acad. Sci. U.S.A.* **2006**, *103*, 10577−10583.

(6) Jürgens, B.; Borchert, H.; Ahrenstorf, K.; Sonström, P.; Pretorius, A.; Schowalter, M.; Gries, K.; Zielasek, V.; Rosenauer, A.; Weller, H.; Bäumer, M. Colloidally prepared nanoparticles for the synthesis of structurally well-defined and highly active heterogeneous catalysts. *Angew. Chem., Int. Ed.* **2008**, *47*, 8946−8949.

(7) Rioux, R. M.; Song, H.; Hoefelmeyer, J. D.; Yang, P.; Somorjai, G. A. High-surface-area catalyst design: Synthesis, characterization, and reaction studies of platinum nanoparticles in mesoporous SBA-15 silica. *J. Phys. Chem. B* **2005**, *109*, 2192−2202.

(8) Song, H.; Rioux, R. M.; Hoefelmeyer, J. D.; Komor, R.; Niesz, K.; Grass, M.; Yang, P.; Somorjai, G. A. Hydrothermal growth of mesoporous SBA-15 silica in the presence of PVP-stabilized Pt nanoparticles: Synthesis, characterization, and catalytic properties. *J. Am. Chem. Soc.* **2006**, *128*, 3027−3037.

(9) Costi, R.; Saunders, A. E.; Banin, U. Colloidal hybrid nanostructures: A new type of functional materials. *Angew. Chem., Int. Ed.* **2010**, *49*, 2−22.

(10) Quan, Z.; Wang, Y.; Fang, J. High-index faceted noble metal nanocrystals. *Acc. Chem. Res.* **2013**, *46*, 191−202.

(11) Park, J. C.; Song, H. Metal@silica yolk-shell nanostructures as versatile bifunctional nanocatalysts. *Nano Res.* **2011**, *4*, 33−49.

(12) Giersig, M.; Ung, T.; Liz-Marzán, L. M.; Mulvaney, P. Direct observation of chemical reactions in silica-coated gold and silver nanoparticles. *Adv. Mater.* **1997**, *9*, 570−575.

(13) Zhang, Q.; Lee, I.; Joo, J. B.; Zaera, F.; Yin, Y. Core-shell nanostructured catalysts. *Acc. Chem. Res.* **2013**, *46*, 1816−1824.

(14) Liu, J.; Qiao, S. Z.; Chen, J. S.; Lou, X. W.; Xing, X.; Lu, G. Q. Yolk/shell nanoparticles: New platforms for nanoreactors, drug

DOI: 10.1021/ar500411s
Acc. Chem. Res. 2015, 48, 491−499

delivery and lithium-ion batteries. *Chem. Commun.* **2011**, *47*, 12578−12591.
(15) Bell, A. T. The impact of nanoscience on heterogeneous catalysis. *Science* **2003**, *299*, 1688−1691.
(16) Yin, Y.; Rioux, R. M.; Erdonmez, C. K.; Hughes, S.; Somorjai, G. A.; Alivisatos, A. P. Formation of hollow nanocrystals through the nanoscale Kirkendall effect. *Science* **2004**, *304*, 711−714.
(17) Lee, J.; Park, J. C.; Song, H. A nanoreactor framework of a Au@SiO_2 yolk/shell structure for catalytic reduction of *p*-nitrophenol. *Adv. Mater.* **2008**, *20*, 1523−1528.
(18) Hervés, P.; Pérez-Lorenzo, M.; Liz-Marzán, L. M.; Dzubiella, J.; Lu, Y.; Ballauff, M. Catalysis by metallic nanoparticles in aqueous solution: Model reactions. *Chem. Soc. Rev.* **2012**, *41*, 5577−5587.
(19) Park, J. C.; Lee, H. J.; Kim, J. Y.; Park, K. H.; Song, H. Catalytic hydrogen transfer of ketones over Ni@SiO_2 yolk−shell nanocatalysts with tiny metal cores. *J. Phys. Chem. C* **2010**, *114*, 6381−6388.
(20) Park, J. C.; Heo, E.; Kim, A.; Kim, M.; Park, K. H.; Song, H. Extremely active Pd@pSiO_2 yolk−shell nanocatalysts for Suzuki coupling reactions of aryl halides. *J. Phys. Chem. C* **2011**, *115*, 15772−15777.
(21) Lee, J.; Park, J. C.; Bang, J. U.; Song, H. Precise tuning of porosity and surface functionality in Au@SiO_2 nanoreactors for high catalytic efficiency. *Chem. Mater.* **2008**, *20*, 5839−5844.
(22) Kim, M.; Park, J. C.; Kim, A.; Park, K. H.; Song, H. Porosity control of Pd@SiO_2 yolk-shell nanocatalysts by the formation of nickel phyllosilicate and its influence on Suzuki coupling reactions. *Langmuir* **2012**, *28*, 6441−6447.
(23) Park, J. C.; Bang, J. U.; Lee, J.; Ko, C. H.; Song, H. Ni@SiO_2 yolk−shell nanoreactor catalysts: High temperature stability and recyclability. *J. Mater. Chem.* **2010**, *20*, 1239−1246.
(24) Park, J. C.; Lee, H. J.; Jung, H. S.; Kim, M.; Kim, H. J.; Park, K. H.; Song, H. Gram-scale synthesis of magnetically separable and recyclable Co@SiO_2 yolk-shell nanocatalysts for phenoxycarbonylation reactions. *ChemCatChem* **2011**, *3*, 755−760.
(25) Park, J. C.; Kim, J. Y.; Heo, E.; Park, K. H.; Song, H. Platinum-centered yolk-shell nanostructure formation by sacrificial nickel spacers. *Langmuir* **2010**, *26*, 16469−16473.
(26) Zhang, Q.; Zhang, T.; Ge, J.; Yin, Y. Permeable silica shell through surface-protected etching. *Nano Lett.* **2008**, *8*, 2867−2871.
(27) Liu, J.; Qiao, S. Z.; Hartono, S. B.; Lu, G. Q. Monodisperse yolk-shell nanoparticles with a hierarchical porous structure for delivery vehicles and nanoreactors. *Angew. Chem., Int. Ed.* **2010**, *49*, 4981−4985.
(28) Kamata, K.; Lu, Y.; Xia, Y. Synthesis and characterization of monodispersed core−shell spherical colloids with movable cores. *J. Am. Chem. Soc.* **2003**, *125*, 2384−2385.
(29) Harada, T.; Ikeda, S.; Ng, Y. H.; Sakata, T.; Mori, H.; Torimoto, T.; Matsumura, M. Rhodium nanoparticle encapsulated in a porous carbon shell as an active heterogeneous catalyst for aromatic hydrogenation. *Adv. Funct. Mater.* **2008**, *18*, 2190−2196.
(30) Arnal, P. M.; Comotti, M.; Schüth, F. High-temperature-stable catalysts by hollow sphere encapsulation. *Angew. Chem., Int. Ed.* **2006**, *45*, 8224−8227.
(31) Lee, I.; Joo, J. B.; Yin, Y.; Zaera, F. A yolk@shell nanoarchitecture for Au/TiO_2 catalysts. *Angew. Chem., Int. Ed.* **2011**, *50*, 10208−10211.
(32) Joo, S. H.; Park, J. Y.; Tsung, C.-K.; Yamada, Y.; Yang, P.; Somorjai, G. A. Thermally stable Pt/mesoporous silica core-shell nanocatalysts for high-temperature reactions. *Nat. Mater.* **2009**, *8*, 126−131.
(33) Cargnello, M.; Delgado Jaén, J. J. D.; Hernández Garrido, J. C.; Bakhmutsky, K.; Montini, T.; Calvino Gámez, J. J.; Gorte, R. J.; Fornasiero, P. Exceptional activity for methane combustion over modular Pd@CeO_2 subunits on functionalized Al_2O_3. *Science* **2012**, *337*, 713−717.
(34) Park, J. C.; Lee, H. J.; Bang, J. U.; Park, K. H.; Song, H. Chemical transformation and morphology change of nickel−silica hybrid nanostructures via nickel phyllosilicate. *Chem. Commun.* **2009**, 7345−7347.
(35) Park, J. C.; Kim, A. Y.; Kim, J. Y.; Park, S.; Park, K. H.; Song, H. ZnO-CuO core-branch nanocatalysts for ultrasound-assisted azide-alkyne cycloadditions reactions. *Chem. Commun.* **2012**, *48*, 8484−8486.
(36) Gao, J.; Gu, H.; Xu, B. Multifunctional magnetic nanoparticles: Design, synthesis, and biomedical applications. *Acc. Chem. Res.* **2009**, *42*, 1097−1107.
(37) Wang, C.; Yin, H.; Dai, S.; Sun, S. A general approach to noble metal-metal oxide dumbbell nanoparticles and their catalytic application for CO oxidation. *Chem. Mater.* **2010**, *22*, 3277−3282.
(38) Kim, M.; Song, H. Precise adjustment of structural anisotropy and crystallinity on metal-Fe_3O_4 hybrid nanoparticles and its influence on magnetic and catalytic properties. *J. Mater. Chem. C* **2014**, *2*, 4997−5004.
(39) Ho, D.; Sun, X.; Sun, S. Monodisperse magnetic nanoparticles for theranostic applications. *Acc. Chem. Res.* **2011**, *44*, 875−882.
(40) Mokari, T.; Rothenberg, E.; Popov, I.; Costi, R.; Banin, U. Selective growth of metal tips onto semiconductor quantum rods and tetrapods. *Science* **2004**, *304*, 1787−1790.
(41) Mokari, T.; Sztrum, C. G.; Salant, A.; Rabani, E.; Banin, U. Formation of asymmetric one-sided metal-tipped semiconductor nanocrystal dots and rods. *Nat. Mater.* **2005**, *4*, 855−863.
(42) Qu, Y.; Duan, X. Progress, challenge and perspective of heterogeneous photocatalysts. *Chem. Soc. Rev.* **2013**, *42*, 2568−2580.
(43) Bang, J. U.; Lee, S. J.; Jang, J. S.; Choi, W.; Song, H. Geometric effect of single or double-tipped CdSe nanorods on photocatalytic H_2 generation. *J. Phys. Chem. Lett.* **2012**, *3*, 3781−3785.
(44) Kim, S. M.; Lee, S. J.; Kim, S. H.; Kwon, S.; Yee, K. J.; Song, H.; Somorjai, G. A.; Park, J. Y. Hot carrier-driven catalytic reactions on Pt-CdSe-Pt nanodumbbells and Pt/GaN under light irradiation. *Nano Lett.* **2013**, *13*, 1352−1358.
(45) Elmalem, E.; Saunders, A. E.; Costi, R.; Salant, A.; Banin, U. Growth of photocatalytic CdSe-Pt nanorods and nanonets. *Adv. Mater.* **2008**, *20*, 4312−4317.
(46) Amirav, L.; Alivisatos, A. P. Photocatalytic hydrogen production with tunable nanorod heterostructures. *J. Phys. Chem. Lett.* **2010**, *1*, 1051−1054.
(47) Skrabalak, S. E.; Chen, J.; Sun, Y.; Lu, X.; Au, L.; Cobley, C. M.; Xia, Y. Gold nanocages: Synthesis, properties, and appplications. *Acc. Chem. Soc.* **2008**, *41*, 1587−1595.
(48) Zeng, J.; Zhang, Q.; Chen, J.; Xia, Y. A comparison study of the catalytic properties of Au-based nanocages, nanoboxes, and nanoparticles. *Nano Lett.* **2010**, *10*, 30−35.
(49) Mahmoud, M. A.; El-Sayed, M. A. Time dependence and signs of the shift of the surface plasmon resonance frequency in nanocages elucidate the nanocatalysis mechanism in hollow nanoparticles. *Nano Lett.* **2011**, *11*, 946−953.
(50) Novo, C.; Funston, A. M.; Mulvaney, P. Direct observation of chemical reactions on single gold nanocrystals using surface plasmon spectroscopy. *Nat. Nanotechnol.* **2008**, *3*, 598−602.
(51) Sambur, J. B.; Chen, P. Approaches to single-nanoparticle catalysis. *Annu. Rev. Phys. Chem.* **2014**, *65*, 395−422.
(52) Langhammer, C.; Larsson, E. M. Nanoplasmonic in situ spectroscopy for catalysis applications. *ACS Catal.* **2012**, *2*, 2036−2045.
(53) Seo, D.; Park, G.; Song, H. Plasmonic monitoring of catalytic hydrogen generation by a single nanoparticle probe. *J. Am. Chem. Soc.* **2012**, *134*, 1221−1227.
(54) Novo, C.; Funston, A. M.; Gooding, A. K.; Mulvaney, P. Electrochemical charging of single gold nanorods. *J. Am. Chem. Soc.* **2009**, *131*, 14664−14666.
(55) Zaera, F. New challenges in heterogeneous catalysis for the 21st century. *Catal. Lett.* **2012**, *142*, 501−516.
(56) Yasukawa, T.; Miyamura, H.; Kobayashi, S. Chiral metal nanoparticle-catalyzed asymmetric C-C bond formation reactions. *Chem. Soc. Rev.* **2014**, *43*, 1450−1461.
(57) Witham, C. A.; Huang, W.; Tsung, C.-K.; Kuhn, J. N.; Somorjai, G. A.; Toste, F. D. Converting homogeneous to heterogeneous in

DOI: 10.1021/ar500411s
Acc. Chem. Res. 2015, 48, 491−499

electrophilic catalysis using monodisperse metal nanoparticles. *Nat. Chem.* **2010**, *2*, 36−41.
(58) Gross, E.; Liu, J. H.-C.; Toste, F. D.; Somorjai, G. A. Control of selectivity in heterogeneous catalysis by tuning nanoparticle properties and reactor residence time. *Nat. Chem.* **2012**, *4*, 947−952.
(59) Kim, M.; Lee, S.; Kim, K.; Shin, D.; Kim, H.; Song, H. A highly Lewis-acidic Pd(IV) surface on Pd@SiO_2 nanocatalysts for hydroalkoxylation reactions. *Chem. Commun.* **2014**, *50*, 14938−14941.
(60) Yamada, Y.; Tsung, C.-K.; Huang, W.; Huo, Z.; Habas, S. E.; Soejima, T.; Aliaga, C. E.; Somorjai, G. A.; Yang, P. Nanocrystal bilayer for tandem catalysis. *Nat. Chem.* **2011**, *3*, 372−376.
(61) Lu, P.; Campbell, C. T.; Xia, Y. A sinter-resistant catalytic system fabricated by maneuvering the selectivity of SiO_2 deposition onto the TiO_2 surface versus the Pt nanoparticle surface. *Nano Lett.* **2013**, *13*, 4957−4962.

DOI: 10.1021/ar500411s
Acc. Chem. Res. 2015, 48, 491−499